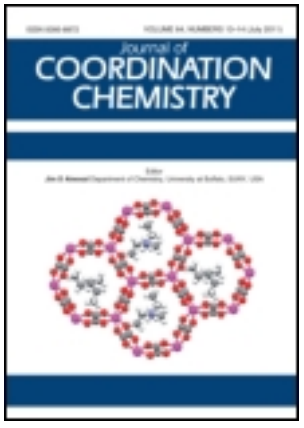

Journal of Coordination Chemistry
Publication details, including instructions for authors and subscription information:
http://www.tandfonline.com/loi/gcoo20

DNA-binding, oxidative DNA cleavage, and coordination mode of later 3d transition metal complexes of a Schiff base derived from isatin as antimicrobial agents

N. Raman [a], K. Pothiraj [a] & T. Baskaran [a]
[a] Research Department of Chemistry, VHNSN College, Virudhunagar - 626001, India
Published online: 08 Nov 2011.

To cite this article: N. Raman, K. Pothiraj & T. Baskaran (2011) DNA-binding, oxidative DNA cleavage, and coordination mode of later 3d transition metal complexes of a Schiff base derived from isatin as antimicrobial agents, Journal of Coordination Chemistry, 64:22, 3900-3917, DOI: 10.1080/00958972.2011.634005

To link to this article: http://dx.doi.org/10.1080/00958972.2011.634005

Journal of Coordination Chemistry
Vol. 64, No. 22, 20 November 2011, 3900–3917

DNA-binding, oxidative DNA cleavage, and coordination mode of later 3d transition metal complexes of a Schiff base derived from isatin as antimicrobial agents

N. RAMAN*, K. POTHIRAJ and T. BASKARAN

Research Department of Chemistry, VHNSN College, Virudhunagar – 626001, India

(*Received 5 July 2011; in final form 11 October 2011*)

A Schiff base, obtained by the condensation of isatin monohydrazone with 2,3,5-trichlorobenzaldehyde, and its Co(II), Ni(II), Cu(II), and Zn(II) complexes have been synthesized and characterized. The interaction of these complexes with DNA is investigated using viscosity, absorption titration, and electrochemical techniques. The results indicate that the complexes bind to Calf thymus DNA through intercalation. Oxidative cleavage activities of the complexes are studied using supercoiled pBR322 DNA by gel electrophoresis. Antimicrobial study reveals that copper and zinc complexes are better antimicrobial agents than the Schiff base and its other complexes.

Keywords: Schiff base; Metal complexes; DNA cleavage; Metal–DNA interaction; Antimicrobial studies

1. Introduction

Various hydrazones which have applications such as biologically active compounds and analytical reagents are obtained depending on the experimental conditions. In analytical chemistry, hydrazones find application in detection, determination, and isolation of compounds containing the carbonyl group [1]. As biologically active compounds, hydrazones find applications in the treatment of diseases, such as antitumor, tuberculosis, leprosy, and mental disorder [2]. Tuberculostatic activity is attributed to the formation of stable chelates with transition metals present in the cell. Recently, a number of attempts have been made to obtain Mn(III), Fe(III), and Co(III) complexes with the bishydrazone formed by the condensation of isatin monohydrazone with 2-hydroxy-1-naphthaldehyde [3].

Isatin, an endogenous indole and its derivatives exhibit a wide range of biological activities [4]. Isatin-based Schiff base copper(II) complex is related to the antiviral drug, methisazone. Significant interest in the design of metal compounds such as drugs and diagnostic agents is termed medicinal inorganic chemistry [5, 6]. Application of electroanalytical techniques includes determination of reaction mechanisms.

*Corresponding author. Email: drn_raman@yahoo.co.in

ISSN 0095-8972 print/ISSN 1029-0389 online
http://dx.doi.org/10.1080/00958972.2011.634005

Redox properties of a drug can give insights into its metabolic fate or pharmaceutical activity [7–9].

Interest in preparation of new metal complexes for interaction with DNA has arisen for applications in biotechnology and medicine. Metal complexes bind to DNA by non-covalent interactions such as electrostatic binding, groove binding, and intercalation [10–12]. Among these interactions, intercalation is an important DNA-binding mode, related to the antitumor activity of the compound [13]. The intercalating ability of the complex depends on the planarity of ligands, the coordination geometry, ligand donor type, and the metal ion type [14]. Copper is a biologically relevant element and many enzymes that depend on copper for their activity have been identified. Because of its biological relevance, a large number of copper(II) complexes have been explored for their biological activities [15, 16]. Many techniques have been applied for investigation of biological efficiencies of metal complexes. Compounds having ability to bind and cleave double stranded DNA under physiological conditions are of importance for their utility as diagnostic agents in medicinal applications and for genomic research [17]. DNA cleavage reactions generally proceed *via* oxidative or hydrolytic cleavage pathways. The hydrolytic pathway involves phosphodiester bond hydrolysis leading to the formation of fragments that could be relegated through enzymatic processes. The oxidative process results in nucleobase oxidation and/or degradation of sugar by abstraction of sugar hydrogen atoms [18].

Although much attention has been directed to metal complexes of the Schiff base derived from isatin [19], no investigations have appeared describing metal complexes of the Schiff base derived from isatin monohydrazone and 2,3,5-trichlorobenzaldehyde. The free ligand and its complexes have been tested for *in vitro* antimicrobial activity against four different bacteria and four different fungi by minimum inhibitory concentration (MIC). The interaction of the complexes with DNA and the evaluation of the binding constants have been explored. The probable binding mode of complexes with DNA and their DNA-damaging properties have been deduced.

2. Experimental

2.1. *Reagents and equipments*

All chemicals were purchased from commercial sources and used as received without purification. The isatin monohydrazone was prepared according to the literature procedure [20]. Supercoiled plasmid (SC) pBR322 DNA and Tris-HCl buffer were purchased from Bangalore Genei (India). Calf thymus DNA (CT-DNA), agarose (molecular biology grade), and ethidium bromide (EB) were obtained from Sigma (USA). Tris-HCl buffer was prepared using deionized and sonicated triply distilled water. Solvents used for electrochemical and spectral measurements were purified by reported procedures [21].

Carbon, hydrogen, and nitrogen analyses of the ligand and complexes were carried out on a CHN analyzer Carlo Erba 1108, Heraeus. Infrared spectra (4000–400 cm^{-1} KBr discs) of the samples were recorded on a Perkin-Elmer 783 series FT-IR spectrophotometer. The electronic absorbance spectra from 200 to 1100 nm were recorded on an UV-1601 spectrophotometer (Shimadzu). ^{1}H NMR spectra of ligand

and its zinc complex (300 MHz) were recorded on a Bruker Avance DRX-300 FT-NMR spectrometer using $CDCl_3$ and DMSO-d_6 as solvents, respectively. Tetramethylsilane was used as internal standard. Chemical shifts were reported in δ scale. EPR spectra of complex in solid state at 300 K and in frozen DMSO at 77 K were recorded on a Varian E-112 spectrometer at X-band, using TCNE as marker with 100 kHz modulation frequency and 9.1 GHz microwave frequency. Mass spectrometry experiments were performed on a JEOL-AccuTOF JMS-T100LC mass spectrometer equipped with a custom-made electrospray interface (ESI). Molar conductances of 10^{-3} molL^{-1} solution of the complexes in DMF were measured at room temperature with a Deep Vision Model-601 digital direct reading deluxe conductivity meter. Magnetic susceptibility measurements were carried out by employing the Gouy method at room temperature on powder sample of the complex. $CuSO_4 \cdot 5H_2O$ was used as calibrant. The metal contents of the complexes were determined according to the literature method [22].

2.2. *DNA-binding and cleavage studies*

2.2.1. Electronic absorption spectral studies. DNA-binding experiments were performed in Tris-HCl/NaCl buffer (5 mmol L^{-1} Tris–HCl/50 mmol L^{-1} NaCl buffer, pH 7.2) using DMF (10%) solution of metal complexes. The concentration of CT-DNA was determined from the absorption intensity at 260 nm with a ε value of 6600 (mol L^{-1})$^{-1}$ cm^{-1} [23]. Absorption titration experiments were made using different concentrations of CT-DNA, while keeping the complex concentration constant. Correction was made for the absorbance of the CT-DNA itself. Samples were equilibrated before recording each spectrum. For metal complexes, the intrinsic binding constant (K_b) was determined from the spectral titration data using the following equation [24]:

$$[\text{DNA}]/(\varepsilon_a - \varepsilon_f) = [\text{DNA}]/(\varepsilon_b - \varepsilon_f) + 1/K_b(\varepsilon_b - \varepsilon_f),$$

where [DNA] is the concentration of DNA in base pairs, the apparent absorption coefficients ε_a, ε_f, and ε_b correspond to A_{obsd}/[Complex], the extinction coefficient of the free complex and the extinction coefficient of the complex when fully bound to DNA, respectively. K_b is the equilibrium binding constant in (mol L^{-1})$^{-1}$. Each sample solution was scanned from 200 to 500 nm.

2.2.2. Electrochemical studies. Cyclic voltammetry was carried out on a CH instrument electrochemical analyzer. All voltammetric experiments were performed in a single compartment cell of volume 10–15 mL containing a three electrode system comprising a glassy carbon working electrode, Pt-wire as auxiliary electrode, and an Ag/AgCl electrode as reference electrode. The supporting electrolyte was 5 mmol L^{-1} Tris-HCl/50 mmol L^{-1} NaCl buffer (pH 7.2). Deaerated solutions were used by purging N_2 gas for 15 min prior to measurements.

2.2.3. Viscosity measurements. Viscosity experiments were conducted on an Ubbelodhe viscometer, immersed in a thermostated water-bath maintained at 37°C. DNA samples with an approximate average length of 200 base pairs were prepared by

sonication in order to minimize complexities arising from DNA flexibility [25]. Titrations were performed for all four complexes (2–12 μmol L^{-1}), and each complex was introduced into the CT-DNA solution (10×10^{-5} mol L^{-1}) present in the viscometer. Data were presented as $(\eta/\eta_0)^{1/3}$ *versus* the ratio of the concentration of the complex to CT-DNA, where η is the viscosity of CT-DNA in the presence of the complex, and η_0 is the viscosity of CT-DNA alone. Viscosity values were calculated from the observed flow time of CT-DNA containing solutions corrected from the flow time of buffer alone (t_0), $\eta = (t - t_0)/t_0$.

2.2.4. Cleavage of pBR322 DNA. The DNA cleavage activity of the complexes was studied by using agarose gel electrophoresis. SC pBR322 DNA (0.3 μg), dissolved in 5 mmol L^{-1} Tris-HCl/50 mmol L^{-1} NaCl buffer (pH 7.2), was treated with the complexes. The mixture was incubated at 37°C for 24 h and then mixed with the loading buffer (2 μL) containing 25% bromophenol blue, 0.25% xylene cyanol, and 30% glycerol. Each sample (5 μL) was loaded into 0.8%(w/v) agarose gel. Electrophoresis was undertaken for 2 h at 50 V in Tris-acetate-EDTA (TAE) buffer (pH 8.0). The gel was stained with EB for 5 min after electrophoresis, and then photographed under UV light. To enhance the DNA cleaving ability by the complexes, hydrogen peroxide (100 μmol L^{-1}) was added into each sample. The cleavage mechanism was further investigated by using the hydroxyl radical scavenger ethanol (4 μL) and the superoxide anion radical scavenger, superoxide dismutase (SOD, 4Units). All experiments were carried out in triplicate under the same conditions.

2.3. *Antimicrobial analyses*

The synthesized ligand and corresponding metal(II) complexes were screened *in vitro* for their antimicrobial activity against *Staphylococcus aureus*, *Escherichia coli*, *Bacillus subtilis,* and *Pseudomonas aeruginosa* bacterial strains and *Aspergillus niger*, *Rhizopus stolonifer*, *Rhizoctonia bataicola*, and *Candida albicans* fungal strains using the agar well diffusion method [26]. The complexes were stored dry at room temperature and dissolved in DMF (10 mgmL^{-1}). Each bacterium was suspended and diluted to *ca* 10^6 cfu mL^{-1}. They were flood inoculated onto the surface of Mueller–Hinton agar (MHA). For fungi, dilution was prepared as 10^6 cfu mL^{-1} and they were flood inoculated onto the surface of potato dextrose agar (PDA). The wells (7.5 mm in diameter) were cut from the agar and 100 μL of each stock complex solution was delivered into them. The plates were then incubated at 37°C for 24 h and 48 h for bacteria and fungi, respectively. Streptomycin and nystatin were used as standards for antibacterial and antifungal drugs, respectively. Inhibitory activity of DMF was also tested in the same way. The antimicrobial activities of the complexes were evaluated by measuring the inhibition-zone diameter observed. MIC was determined by the broth dilution technique according to the National Committee for Clinical Laboratory Standard [27]. The lowest concentration (highest dilution) required to arrest the growth of bacteria was regarded as MIC.

2.4. *Preparation of Schiff base (L)*

The synthesis of L is schematically presented in scheme 1. The Schiff base has been synthesized by refluxing hot methanolic solution (50 mL) of 2,3,5-trichlorobenzaldehyde (2.09 g, 10 mmol) and hot methanolic solution (40 mL) of isatin monohydrazone

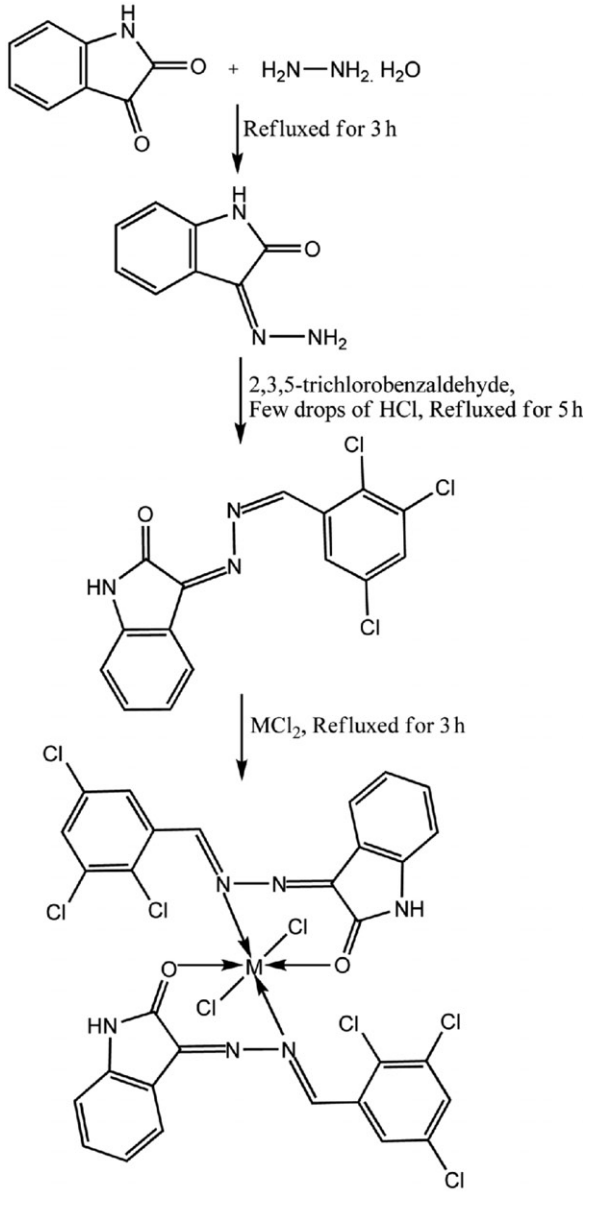

Scheme 1. The synthesis of the Schiff base ligand and its metal(II) complexes.

(1.61 g, 10 mmol) for 5 h with a few drops of hydrochloric acid. The product obtained after evaporation of the solvent was filtered and washed with cold methanol.

$C_{15}H_8N_3OCl_3$: Yield (%): 75.38, dark red, m.p.: 258°C, m.wt: 352.60. Anal. Calcd (%): C, 51.10; H, 2.29; N, 11.92; Cl, 30.16. Found (%): C, 50.98; H, 2.25; N, 11.88; Cl, 30.11; ^{1}H NMR ($CDCl_3$, δ/ppm): 6.91–7.94 (m, 6H, Ar–H), 8.91 (s, 1H, CH=N), 9.83 (s, 1H, NH); IR (KBr, ν/cm^{-1}): 3283 ν(NH), 3060 ν(Ar–CH), 1722 ν(C=O), 1645 ν(C=N), 1614 ν[(CH=N)(azomethine)], 1543 ν(Ar–C=C), 993 ν(NN). UV-Vis (DMF, λ_{max}/nm): 225, 339, and 384.

2.5. *Preparation of Co(II), Ni(II), Cu(II), and Zn(II) complexes*

Hot methanolic solution (25 mL) of Schiff base (0.705 g, 2 mmol) was mixed with hot methanolic solution (15 mL) of $CoCl_2 \cdot 6H_2O$ (0.237 g, 1 mmol)/$NiCl_2 \cdot 6H_2O$ (0.237 g, 1 mmol)/$CuCl_2 \cdot 2H_2O$ (0.170 g, mmol)/$ZnCl_2$ (0.136 g, 1 mmol) and refluxed on a water bath for 3 h. The separated complex was filtered, washed thoroughly with water and methanol, and dried in vacuum over fused $CaCl_2$.

[$CoC_{30}H_{16}N_6O_2Cl_8$]: Yield (%): 72.15, reddish brown, m.p.: 228°C, m.wt: 835.05. Anal. Calcd (%): Co, 7.06; C, 43.15; H, 1.93; N, 10.06; Cl, 33.96. Found (%): Co, 7.02; C, 43.07; H, 1.91; N, 9.98; Cl, 33.67; IR (KBr, ν/cm^{-1}): 3284 ν(NH), 3058 ν(Ar–CH), 1705 ν(C=O), 1644 ν(C=N), 1603 ν[(CH=N)(azomethine)], 1545 ν(Ar–C=C), 1003, ν(NN), 570 ν(Co–O), 435 ν(Co–N); UV-Vis (DMF, λ_{max}/nm): 229, 352, 401, 603, and 684; molar conductance (DMF): 7.68 Ω^{-1} cm^2 mol^{-1}; μ_{eff} (BM): 4.82.

[Ni $C_{30}H_{16}N_6O_2Cl_8$]: Yield (%): 70.20, light red, m.p.: 235°C, m.wt: 834.81. Anal. Calcd (%): Ni, 7.03; C, 43.16; H, 1.93; N, 10.07; Cl, 33.97. Found (%): Ni, 6.95; C, 43.12; H, 1.88; N, 10.01; Cl, 33.85; IR (KBr, ν/cm^{-1}): 3282 ν(NH), 3056 ν(Ar–CH), 1706 ν(C=O), 1643 ν(C=N), 1605 ν[(CH=N)(azomethine)], 1548 ν(Ar–C=C), 1001, ν(NN), 560 ν(Ni–O), 440 ν(Ni – N); UV-Vis (DMF, λ_{max}/nm): 233, 351, 402, 485, 624, and 772; molar conductance (DMF): 1.28 Ω^{-1} cm^2 mol^{-1}; μ_{eff} (BM): 3.08.

[$CuC_{30}H_{16}N_6O_2Cl_8$]: Yield (%): 71.85, brown, m.p.: 217°C, m.wt: 839.66. Anal. Calcd (%): Cu, 7.57; C, 42.91; H, 1.92; N, 10.01; Cl, 33.78. Found (%): Cu, 7.46; C, 42.83; H, 1.89; N, 9.95; Cl, 33.72. IR (KBr, ν/cm^{-1}): 3282 ν(NH), 3059 ν(Ar–CH), 1710 ν(C=O), 1645 ν(C=N), 1599 ν[(CH=N)(azomethine)], 1544 ν(Ar–C=C), 1002 ν(NN), 565 ν(Cu–O), 430 ν(Cu–N); UV-Vis (DMF, λ_{max}/nm): 230, 354, 400, 538, 615, and 768; molar conductance (DMF): 5.45 Ω^{-1} cm^2 mol^{-1}; μ_{eff} (BM): 1.98.

[$ZnC_{30}H_{16}N_6O_2Cl_8$]: Yield (%): 71.28, reddish yellow, m.p.: 240°C, m.wt: 841.51. Anal. Calcd (%): Zn, 7.77; C, 42.82; H, 1.92; N, 9.99; Cl, 33.70. Found (%): Zn, 7.71; C, 42.79; H, 1.85; N, 9.93; Cl, 33.65. ^{1}H NMR (DMSO-d_6, δ/ppm): 6.89–7.93 (m, 12H, Ar–H), 8.51 (s, 2H, CH=N), 9.82 (s, 2H, NH); IR (KBr, ν/cm^{-1}): 3284 ν(NH), 3058 ν(Ar–CH), 1708 ν(C=O), 1644 ν(C=N), 1603 ν[(CH=N)(azomethine)], 1547 ν(Ar–C=C), 1005, ν(NN), 562 ν(Zn–O), 425 ν(Zn–N); UV-Vis (DMF, λ_{max}/nm): 231, 348, and 402; molar conductance (DMF): 12.45 Ω^{-1} cm^2 mol^{-1}; μ_{eff} (BM): diamagnetic.

3. Results and discussion

Spectroscopic studies and analytical data support the proposed structure of the ligand and its metal complexes (scheme 1). Ligand (L) is soluble in many organic solvents but complexes are soluble only in DMSO and DMF. Molar conductance measurements in DMF show that complexes are non-electrolytes.

3.1. *IR spectra*

The functional groups of the Schiff base and the metal complexes were detected by infrared spectra. Spectral features of the complexes were strikingly similar, but were different from those of the ligand. In spectra of the complexes, the band due to the aldimine ν(CH=N) shifted to lower frequency by 9–15 cm^{-1}, indicating its involvement in chelation with metal [28]. However, the band corresponding to ketimine remained almost unaffected, indicating nonparticipation in bond formation with metal. The band corresponding to ν(C=O) shifted to lower frequency by 12–17 cm^{-1} in the metal complexes, suggesting its coordination with metal. The high intensity band at 1643–1645 cm^{-1} in the IR spectra of the Schiff base and its metal complexes was assigned to ν(C=N) for ketimine. The IR spectrum of the Schiff base exhibited band due to ν(NH) at 3282–3284 cm^{-1}. The unaltered positions of ν(NH) and ν(C=N) in the metal complexes indicated that these groups were not involved in coordination. New bands at 425–440 and 560–570 cm^{-1} in spectra of the complexes were assigned to stretching frequencies of M–N and M–O, respectively [29]. Thus, the IR spectral results provide evidence for bidentate complexation of Schiff base with metal.

3.2. *Electronic spectral analysis and magnetic properties*

Electronic spectra of the Schiff base and its complexes were recorded in DMF. The absorption maxima and magnetic moment data of the complexes are listed in table 1.

Table 1. Electronic absorption spectral data, magnetic moments, and molar conductances of metal(II) complexes at room temperature.

Complex	λ_{max} (nm)	Band assignments	Geometry	Magnetic moment (BM)	Molar conductance ($\Omega^{-1}\,cm^2\,mol^{-1}$)
$[CoL_2Cl_2]$	603	$^4T_{Ig}(F) \rightarrow {}^4T_{Ig}(P)$			
	684	$^4T_{1g}(F) \rightarrow {}^4A_{2g}(F)$	Octahedral	4.82	7.68
$[NiL_2Cl_2]$	485	$^3A_{2g}(F) \rightarrow {}^3T_{1g}(P)$			
	624	$^3A_{2g}(F) \rightarrow {}^3T_{1g}(F)$	Octahedral	3.08	1.28
	772	$^3A_{2g}(F) \rightarrow {}^3T_{2g}(F)$			
$[CuL_2Cl_2]$	538	$^2B_{1g} \rightarrow {}^2B_{2g}$			
	615	$^2B_{1g} \rightarrow {}^2E_g$	Octahedral	1.98	5.45
	768	$^2B_{1g} \rightarrow {}^2A_{2g}$			
$[ZnL_2Cl_2]$	231	INCT			
	348	INCT	–	Diamagnetic	12.45
	402	MLCT			

The Schiff base showed strong bands at 225, 339, and 384 nm due to π–π^* and n–π^* transitions [30].

The electronic spectrum of Co(II) complex exhibited bands at 603 ($\varepsilon = 182\,dm^3\,(mol\,L^{-1})^{-1}\,cm^{-1}$) and 684 nm ($\varepsilon = 148\,dm^3\,(mol\,L^{-1})^{-1}\,cm^{-1}$), assigned to $^4T_{Ig}(F) \rightarrow {}^4T_{Ig}(P)$ and $^4T_{1g}(F) \rightarrow {}^4A_{2g}(F)$ transitions, respectively, corresponding to octahedral geometry around Co(II) [31]. The observed magnetic moment of 4.82 BM for Co(II) complemented the electronic spectral findings [32].

The electronic spectrum of Ni(II) complex exhibited three bands at 485 ($\varepsilon = 160\,dm^3\,(mol\,L^{-1})^{-1}\,cm^{-1}$), 624 ($\varepsilon = 134\,dm^3\,(mol\,L^{-1})^{-1}\,cm^{-1}$) and 772 nm ($\varepsilon = 102\,dm^3\,(mol\,L^{-1})^{-1}\,cm^{-1}$), attributed to $^3A_{2g}(F) \rightarrow {}^3T_{1g}(P)$, $^3A_{2g}(F) \rightarrow {}^3T_{1g}(F)$ and $^3A_{2g}(F) \rightarrow {}^3T_{2g}(F)$ transitions, respectively, characteristic of an octahedral Ni(II) complex, which was further supported by its magnetic moment of 3.08 BM [31, 32].

The electronic spectrum of the Cu(II) complex reported here showed three bands at 538 ($\varepsilon = 98\,dm^3\,(mol\,L^{-1})^{-1}\,cm^{-1}$), 615 ($\varepsilon = 84\,dm^3\,(mol\,L^{-1})^{-1}\,cm^{-1}$) and 768 nm ($\varepsilon = 63\,dm^3\,(mol\,L^{-1})^{-1}\,cm^{-1}$), assigned to $^2B_{1g} \rightarrow {}^2B_{2g}$, $^2B_{1g} \rightarrow {}^2E_g$, and $^2B_{1g} \rightarrow {}^2A_{2g}$ transitions, respectively. The magnetic moment of 1.98 BM was higher than the spin-only value (1.73 BM) expected for one unpaired electron and offered the possibility of an octahedral geometry. The Zn(II) complex was diamagnetic and from the empirical formula of this complex, an octahedral geometry was proposed [33, 34].

3.3. *Molar conductivity measurements*

The molar conductivities of metal(II) complexes in DMF ($10^{-3}\,mol\,L^{-1}$) are given in table 1. The conductance values measured ($1.28–12.45\,\Omega^{-1}\,cm^2\,mol^{-1}$) were too low to account for dissociation and hence the complexes were considered as non-electrolytes.

3.4. *^{1}H NMR spectral analysis*

The ^{1}H NMR spectrum of the free ligand showed peaks at 9.83 and 8.91 ppm, assigned to (NH) of the indole ring and the azomethine (CH=N), respectively. The aromatic ring protons of both the ligand and its zinc complex were multiplets in the range 6.89–7.94 ppm. However, in the spectrum of zinc complex, the azomethine (CH=N) protons showed an upfield shift to 8.51 ppm, thereby suggesting coordination of imino nitrogen to zinc [35].

3.5. *Mass spectral studies*

The ESI mass spectrum gave additional structural information about the stereochemistry of the studied compounds. The mass spectra were characterized by strong to medium molecular ion peaks, in good accord with their suggested empirical formulae as indicated from elemental analyses. The mass spectrum of the ligand showed a peak at m/z 353 corresponding to $[M]^+$ while the isotopic peaks of chlorine (^{37}Cl) present in the ligand were observed at m/z 355 (M + 2), 357 (M + 4), and 359 (M + 6). The mass spectra of $[CuL_2Cl_2]$, $[CoL_2Cl_2]$, $[NiL_2Cl_2]$, and $[ZnL_2Cl_2]$ complexes showed peaks at m/z 840, 835, 836 (M + 1), and 842 corresponding to the molecular ion peak of the respective complexes and also the isotopic peaks of all the complexes were observed

Table 2. Spin Hamiltonian parameters of Cu(II) complex in DMSO solution.

	g-tensors			Hyperfine constant $\times 10^{-4}$ cm^{-1}			Bonding parameters							
Complex	$g_\parallel$	$g_\perp$	g_{av}	$A_\parallel$	$A_\perp$	A_{av}	$g_\parallel/A_\parallel$	G	α^2	β^2	γ^2	$K_\parallel$	$K_\perp$	K
$[CuL_2Cl_2]$	2.26	2.05	2.15	130	90	106.66	173.84	5.43	0.68	0.92	0.68	0.63	0.46	0.33

with the weak relative intensities at (M + 2), (M + 4), (M + 6), (M + 8), (M + 10), (M + 12), (M + 14), and (M + 16). In all the complexes, the observed fragment ions $[C_{30}H_{16}N_6Cl_7O_2M]^{+\cdot}$ and $[C_{30}H_{16}N_6Cl_6O_2M]^+$ were due to elimination of two coordinated chlorides one by one. All complexes gave a few unstable fragment ions, namely $[C_{15}H_8N_3Cl_3O]^+$, $[C_7H_3NCl_3]^+$, and $[C_6H_2Cl_3]^+$. Mass spectra of the ligand and its complexes are given in "Supplementary material" (figures S1–S5). The mass spectral and elemental analyses reveal that the complexes are monomeric.

3.6. *Electron paramagnetic resonance spectra*

X-band EPR spectra of the polycrystalline copper complex recorded in DMSO at 300 K (RT) and 77 K (LNT) are given in "Supplementary material" (figures S6 and S7). The spin Hamiltonian parameters calculated are given in table 2. The spectrum of the complex at 300 K showed one intense absorption at high field and was isotropic due to tumbling motion of the molecules. The EPR spectrum of the Cu(II) complex in DMSO at 77 K showed well-resolved hyperfine spectra giving $g_\parallel > g_\perp > 2.0027$, corresponding to the presence of an unpaired electron in the $d_{x^2-y^2}$ orbital. For a Cu(II) complex, $g_\parallel$ is a parameter sensitive enough to indicate covalence. The fact that $g_\parallel$ is less than 2.3 is an indication of significant covalent character to the M–L bond [36].

The geometric parameter G, which is a measure of exchange interaction between the copper centre in polycrystalline compounds, was calculated using the equation $G = (g_\parallel - 2.0027)/(g_\perp - 2.0027)$. According to Hathaway [37, 38], if the value of G is greater than four, the exchange interaction between Cu(II) centers in the solid state is negligible, whereas when it is less than four, a considerable exchange interaction is indicated in the solid complex. The calculated G value is 5.43 for the present copper complex indicating that magnetic interaction between Cu(II) ions is negligible in the solid complex [39].

The EPR parameters $g_\parallel$, $g_\perp$, g_{av}, g_{av}, $A_\parallel$, and $A_\perp$ for copper complex and the energies of d–d transitions were used to evaluate the bonding parameters α^2, β^2, and γ^2, which may be regarded as measure of the covalency of the in-plane σ-bonding and the in-plane π- and out-of-plane π-bonding, respectively. The value of in-plane σ-bonding parameter α^2 was calculated using the expression [40].

$$\alpha_2 = -(A_{||}/0.036) + (g_{||} - 2.0027) + (3/7)(g_\perp - 2.0027) + 0.04.$$

The following simplified expressions were used to calculate the bonding parameters [41].

$$K_{||}^2 = (g_{||} - 2.0027)E_{d-d}/8\lambda_0,$$
$$K_\perp^2 = (g_\perp - 2.0027)E_{d-d}/2\lambda_0,$$

where $K_{\parallel} = \alpha^2\beta^2$, $K_{\perp} = \alpha^2\gamma^2$, and λ_0 represents the one electron spin-orbit coupling constant for the free ion, equal to $-828\,cm^{-1}$. Hathaway [42] has pointed out that for pure σ-bonding $K_{\parallel} \approx K_{\perp} \approx 0.77$ and for in-plane π-bonding, $K_{\parallel} < K_{\perp}$, while for out-of-plane π-bonding $K_{\perp} < K_{\parallel}$. In the present copper complex, $K_{\parallel} > K_{\perp}$ indicates the presence of significant out-of-plane π-bonding. Furthermore α^2, β^2, and γ^2 have values less than 1.0, which is expected for 100% ionic character of the bonds and become smaller with increasing covalent bonding. Therefore, the evaluated values of α^2, β^2, and γ^2 of the complex are consistent with both in-plane σ and in-plane π-bonding.

The Fermi contact hyperfine interaction term K may be obtained from [43],

$$K = A_{av}/P\beta^2 + (g_{av} - 2.0027)/\beta^2,$$

where P is the free ion dipolar term and its value is 0.036. K is a dimensionless quantity, which is a measure of the contribution of s electrons to the hyperfine interaction and is generally found to have a value of 0.30. The K value obtained for the copper complex is in agreement with those estimated by Assour [44]. The results of EPR parameters, electronic absorption, and magnetic measurement data revealed that the prepared copper complex has octahedral geometry.

3.7. *Metal–DNA interaction*

Transition metal complexes bind to DNA *via* both covalent and/or non-covalent interactions. In covalent binding the labile ligand of the complexes is replaced by a nitrogen base of DNA such as guanine N7. On the other hand, the non-covalent DNA interactions include intercalation, electrostatic, and groove (surface) binding of metal complexes, outside of the DNA helix, along major or minor grooves [45].

3.7.1. Electronic absorption titration study of the DNA-binding. Electronic absorption spectroscopy was used to study the interaction of metal complexes with DNA [46]. The change in absorbance and shift in wavelength upon addition of increasing concentration of DNA solution in a fixed concentration of metal complexes gives information on the mode of interaction. Metal complex binding with DNA through intercalation usually results in hypochromism and bathochromism due to the strong stacking interaction between the aromatic chromophore and the base pairs of DNA. The DNA-binding constant of metal(II) complexes are usually determined by the MLCT band because no light absorption for DNA is found in the range of wavelength over 395 nm and thus no interference exists. The extent of the hypochromism in the visible MLCT band is consistent with the strength of intercalative interaction [47].

To clarify interactions between the compound and DNA, electronic absorption spectra of the metal complexes in the absence and presence of the CT-DNA (at a constant concentration of the compounds) were obtained; the DNA-binding of copper complex is shown in figure 1. With increasing DNA concentrations, the absorption band at 398 nm of the Co(II) complex represented hypochromism of 12.65%; the absorption band at 401.7 nm of the Ni(II) complex exhibited hypochromism of 19.93%; the absorption band at 400.5 nm of the Cu(II) complex appeared hypochromism of 22.84% and the absorption band at 402.5 nm of the Zn(II) complex appeared hypochromism of 16.71%. The bathochromism of Co(II), Ni(II), Cu(II), and Zn(II)

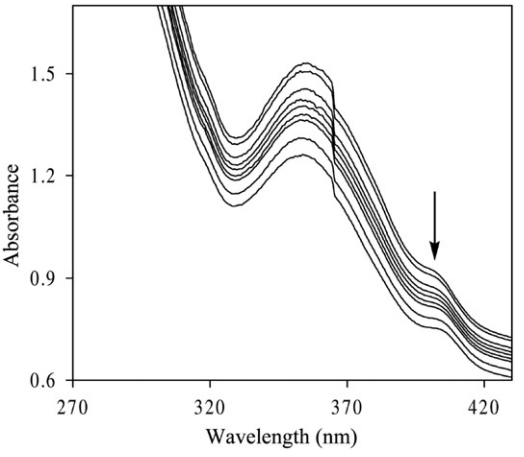

Figure 1. Absorption spectrum of copper(II) complex in the absence and presence of increasing amounts of CT-DNA at room temperature in 50 mmol L^{-1} Tris-HCl/50 mmol L^{-1} NaCl buffer (pH 7.2). Arrow shows the absorbance change upon increasing DNA concentration.

Table 3. Absorption properties of metal(II) complexes.

	λ_{max} (nm)				
Complex	Free	Bound	$\Delta\lambda$ (nm)	Hypochromicity (%)	$K_b \times 10^4$ ((mol L^{-1})$^{-1}$)
$[CoL_2Cl_2]$	398.0	399.5	1.5	12.65	2.54 ± 0.20
$[NiL_2Cl_2]$	401.7	404	2.2	19.93	3.99 ± 0.32
$[CuL_2Cl_2]$	400.5	403.5	3.0	22.84	6.94 ± 0.36
$[ZnL_2Cl_2]$	402.5	404.3	1.8	16.71	3.62 ± 0.28

complexes was shifted to 1.5, 2.2, 3.0, and 1.8 nm, respectively. The hypochromism observed for the $\pi \rightarrow \pi^*$ transition band indicated strong binding of the metal complexes to DNA. The binding constant (K_b) values of the Co(II), Ni(II), Cu(II), and Zn(II) complexes were $2.54 \pm 0.20 \times 10^4$ (mol L^{-1})$^{-1}$, $3.99 \pm 0.32 \times 10^4$ (mol L^{-1})$^{-1}$, $6.94 \pm 0.36 \times 10^4$ (mol L^{-1})$^{-1}$, and $3.62 \pm 0.28 \times 10^4$ (mol L^{-1})$^{-1}$, respectively, which were consistent with hypochromism degree (table 3).

The K_b values obtained here are lower than those reported for classical intercalators (EB and [Ru(phen)(dppz)] whose binding constants are on the order of 10^6–10^7 (mol L^{-1})$^{-1}$) [48, 49] and also compared to other reported later 3d metal complexes ($K_b = 0.88$–3.83×10^4 (mol L^{-1})$^{-1}$). Thus, the synthesized complexes have slightly superior intercalating properties due to containing more electron-releasing substituents and coordinated chlorides [50, 51]. It is clear that the hypochromism and K_b values are not enough evidence, but these results can suggest an intimate association of the compounds with CT-DNA and indicate that the binding strength of complex is in the order Cu(II) complex > Ni(II) complex > Zn(II) complex > Co(II) complex.

3.7.2. Cyclic voltammetry study of the DNA-binding. Electrochemical investigations of metal–DNA interactions provide a useful complement to spectroscopic methods, for

example, for non-absorbing species, and yield information about interactions with both the reduced and oxidized forms of the metal [52]. In figure 2, the cyclic voltammograms of copper complex in the presence of CT-DNA in various concentrations are shown. It has been pointed out that the electrochemical potential of a small molecule will shift positively when it intercalates into DNA double helix, and if it is bound to DNA by electrostatic interaction, the potential would shift in a negative direction [53].

The two quasi-reversible and one irreversible redox couples for Cu(II) complex, one quasi-reversible redox couple for Co(II) complex and only one irreversible redox couple for Zn(II) complex in 1 : 2 DMF : buffer solution that has been studied upon addition of CT-DNA and the shifts of the cathodic (E_{pc}) and anodic (E_{pa}) potentials are given in table 4. No new redox peaks appeared after the addition of CT-DNA to each complex, but the current intensity of all the peaks decreased significantly, suggesting the existence of an interaction between each complex and CT-DNA. The decrease in current intensity can be explained in terms of an equilibrium mixture of free and DNA-bound complexes to the electrode surface [54].

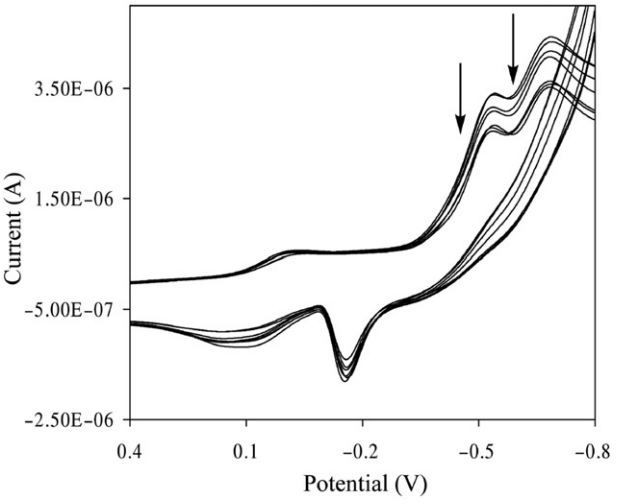

Figure 2. Cyclic voltammogram of copper(II) complex in the absence and presence of increasing amounts of CT-DNA at room temperature in DMF : buffer (1 : 2) mixture (pH 7.2) (scan rate 0.1 V s^{-1}). The arrows show the current changing upon increasing DNA concentration.

Table 4. Electrochemical behavior of metal(II) complexes in the absence and presence of CT-DNA.

		E_{pc} (V)		E_{pa} (V)		ΔE_p (V)		$E_{1/2}$ (V)		
Complex	Redox couple	Free	Bound	Free	Bound	Free	Bound	Free	Bound	K_R/K_O
$[CoL_2Cl_2]$	Co(II)/Co(I)	−0.668	−0.645	−0.305	−0.289	0.363	0.356	−0.973	−0.934	4.56
$[CuL_2Cl_2]$	Cu(III)/Cu(II)	0.018	0.005	0.086	0.107	0.068	0.102	0.104	0.112	1.36
	Cu(II)/Cu(I)	−0.543	−0.535	−0.155	−0.146	0.388	0.389	−0.698	−0.681	1.93
	Cu(I)/Cu(0)	−0.684	−0.690	–	–	–	–	–	–	–
$[ZnL_2Cl_2]$	Zn(II)/Zn(I)	−0.415	−0.369	–	–	–	–	–	–	–

Cu(II), Co(II), and Zn(II) complexes exhibit different electrochemical behavior upon the addition of CT-DNA at various concentrations. For increasing amounts of CT-DNA, the cathodic potentials E_{pc} show a positive shift except copper complex ($\Delta E_{pc} = +13$, $+8$, and -6 mV for copper complex, $\Delta E_{pc} = +35$ mV for cobalt complex and $\Delta E_{pc} = +23$ mV for zinc complex) while the anodic potential E_{pc} shifted to more positive values ($\Delta E_{pa} = +21$ and $+9$ mV for copper complex, $\Delta E_{pa} = +16$ mV for cobalt complex). The shift in $E_{1/2}$ values can be used to estimate the ratio of equilibrium constants, K_R/K_O for binding of M(II) and M(I) forms, respectively, to DNA. For a Nernstian electron transfer system in which both the oxidized and reduced forms are associated with a third species such as DNA in solution can be applied. Here, M^{n+}-DNA represents the metal complexes bound to DNA with $n+$ charge on the metal centre. Thus for a one electron transfer,

$$E_b^\circ - E_f^\circ = 0.0591 \log(K_R/K_O),$$

where E_f° and E_b° are the formal potentials of the M(II)/M(I) couple in the free and bound forms, respectively. K_R and K_O are the corresponding binding constants for the M^{2+} and M^+ species to DNA. For Co(II) and Cu(II) the complexes, K_R is higher than K_O, suggesting that the interaction of metal complexes with DNA tends to stabilize the M(II) over the M(I) state (table 4). Finally, the conclusion derived from the CV study is that copper complex can bind to DNA by both intercalation and electrostatic interaction, while cobalt and zinc complex can bind to DNA by intercalative binding mode [55, 56].

3.7.3. Viscosity measurements. Viscosity titration measurements were carried out to clarify the interaction between the investigated compounds and CT-DNA. It is sensitive to length changes and regarded as the least ambiguous and the most critical test of a binding model in solution in the absence of crystallographic structural data [57]. A classical intercalation model demands that the DNA helix must lengthen as base pairs are separated to accommodate the binding complexes, leading to increase of DNA viscosity [58]. In contrast, a partial and/or non-classical intercalation of the complex could bend (or kink) the DNA helix, reducing its viscosity concomitantly. In addition, some compounds such as $[Ru(bpy)_3]^{2+}$, which interact with DNA by an electrostatic binding mode, have no influence on DNA viscosity [59]. To further elucidate the binding mode of the present complexes, viscosity measurements were carried out by keeping $[DNA] = 10 \times 10^{-5}$ mol L^{-1} and varying the concentration of the compounds. The effects of metal complexes on the viscosities of CT-DNA are shown in figure 3. With the ratios of the investigated compounds to CT-DNA increasing, the relative viscosities of DNA increased steadily, indicating that there exist intercalation between the compounds and DNA helix. The increased degree of viscosity, which may depend on the binding affinity of compounds to DNA, follows the order Cu(II) complex > Ni(II) complex > Zn(II) complex > Co(II) complex. On the basis of the electronic absorption titration and voltammetric studies together with the viscosity measurements, we find that all four metal complexes bind to CT-DNA *via* an intercalative binding mode and the Cu(II) complex binds to CT-DNA more strongly.

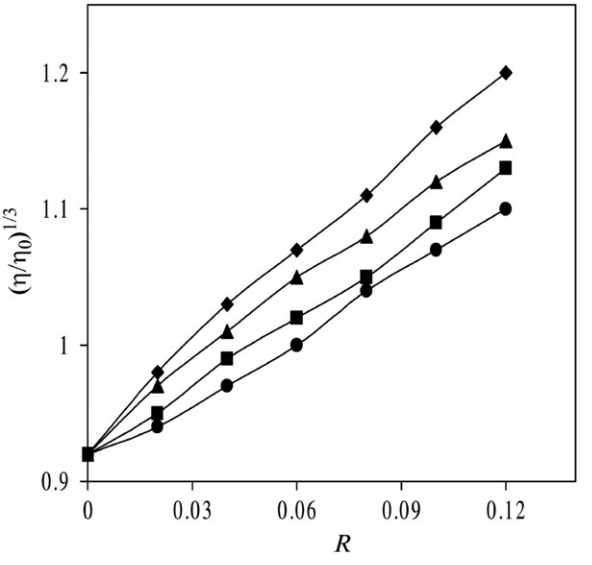

Figure 3. Change in relative specific viscosity of CT-DNA (10×10^{-5} molL^{-1}) on addition of $[CuL_2Cl_2]$ (◆), $[NiL_2Cl_2]$ (▲), $[ZnL_2Cl_2]$ (■) and $[CoL_2Cl_2]$ (●) in 50 mmol L^{-1} Tris–HCl/50 mmol L^{-1} NaCl buffer (pH 7.2) at 37°C, R = [complex]/[DNA].

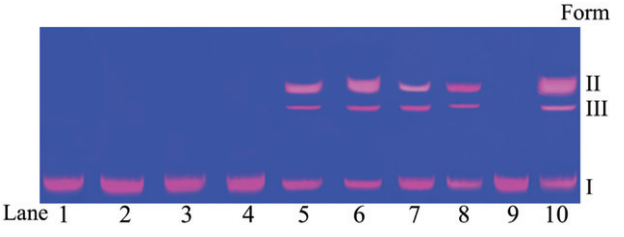

Figure 4. Cleavage of SC pBR322 DNA (0.3 μg) by metal(II) complexes (0.30 mmol L^{-1}) in the presence of hydrogen peroxide (100 μmol L^{-1}) in 50 mmol L^{-1} Tris–HCl/50 mmol L^{-1} NaCl buffer (pH 7.2). Lane 1, DNA control; Lane 2, DNA + H_2O_2; Lane 3, DNA + $[CuL_2Cl_2]$; Lane 4, DNA + ethanol (4 μL); Lanes 5–8, DNA + H_2O_2 + $[CoL_2Cl_2]$, $[CuL_2Cl_2]$, $[ZnL_2Cl_2]$, and $[NiL_2Cl_2]$, respectively; Lane 9, DNA + H_2O_2 + ethanol (4 μL) + $[CuL_2Cl_2]$; Lane 10, DNA + H_2O_2 + SOD (4 Units) + $[CuL_2Cl_2]$.

3.8. *DNA-cleavage studies*

Antitumor agents can interact with DNA and cause DNA strand scission, for this reason we have also studied the capacity to cleave DNA by agarose gel electrophoresis using plasmid pBR322 DNA. The naturally occurring supercoiled form (Form I), when nicked, gives an open circular relaxed form (Form II) and upon further cleavage, results in the linear form (Form III). When subjected to gel electrophoresis, relatively fast migration is observed for Form I. Form II migrates slowly and Form III migrates between Forms I and II. As shown in figure 4, control experiments suggested that untreated DNA, DNA incubated with either peroxide or copper complex alone and in the presence of ethanol with DNA did not show significant DNA cleavage (Lanes 1–4). In the presence of H_2O_2, Form I converted into Form II (nicked DNA) and Form III

Table 5. The *in-vitro* antimicrobial activity of ligand and its metal(II) complexes evaluated by MIC ($\mu g\,mL^{-1}$).

	Antibacterial activity				Antifungal activity			
Complex	*S. aureus*	*B. subtilis*	*E. coli*	*P. aeruginosa*	*A. niger*	*R. bataicola*	*R. stolonifer*	*C. albicans*
Ligand (L)	150	250	100	100	150	200	200	100
$[CoL_2Cl_2]$	75	100	25	50	50	50	75	25
$[NiL_2Cl_2]$	75	75	50	50	75	75	100	50
$[CuL_2Cl_2]$	50	50	20	25	25	20	50	20
$[ZnL_2Cl_2]$	75	100	25	20	20	25	25	20
Streptomycin	5	10	5	10	–	–	–	–
Nystatin	–	–	–	–	5	10	10	10

(linear DNA) (Lanes 5–8), which indicated that all four complexes are potent DNA cleavage agents in the presence of H_2O_2 as an oxidizing agent under the present experimental conditions. The addition of hydroxyl radical scavenger (ethanol) completely inhibited DNA cleavage activity (Lane 9). Moreover, on addition of superoxide anion radical scavenger (SOD), there is no apparent inhibition in the DNA cleavage (Lane 10), suggesting that the cleavage mechanism involves oxidative reactions *via* hydroxyl radical species [60].

3.9. *Antimicrobial evaluation of ligand and its metal complexes*

The ligand and metal complexes were screened for antibacterial activity and the results are presented in table 5. The MIC was determined by assaying using the broth dilution technique. The synthesized Schiff base has an inhibitory effect (MIC values of 100–250 $\mu g\,mL^{-1}$) on growth of the tested bacterial strains. All complexes showed greater bactericidal activities against *E. coli* (MIC 20–50 $\mu g\,mL^{-1}$), *S. aureus* (MIC 50–75 $\mu g\,mL^{-1}$), *P. aeruginosa* (MIC 20–50 $\mu g\,mL^{-1}$) and *B. subtilis* (MIC 50–100 $\mu g\,mL^{-1}$) than the ligand. In the fungal studies, the ligand had an inhibitory effect (MIC values in range 100–200 $\mu g\,mL^{-1}$) on the growth of the tested strains and complexes again showed greater fungicidal activities against *A. niger* (MIC 20–75 $\mu g\,mL^{-1}$), *R. stolonifer* (MIC 25–100 $\mu g\,mL^{-1}$), *R. bataicola* (MIC 20–75 $\mu g\,mL^{-1}$), and *C. albicans* (MIC 20–50 $\mu g\,mL^{-1}$). Cu(II) and Zn(II) complexes had greater bacterial and fungal activities than the ligand. The synthesized complexes, having more electron releasing substituents and two coordinated chlorides, increased the microbial activity as compared to reported isatin-based Schiff base metal complexes [50, 61].

Chelation [62, 63] reduces the polarity of the metal ion considerably, mainly because of the partial sharing of its positive charge with donor groups and possible π-electron delocalization on the whole chelate ring. Lipids and polysaccharides are important constituents of cell walls and membranes, which are preferred for metal ion interaction. The cell wall also contains several aminophosphates, carbonyl, and cysteinyl ligands, which maintain the integrity of the membrane by acting as a diffusion barrier and also provides suitable sites for binding. Chelation reduces not only the polarity of the metal ion, but increases the lipophilic character of the chelate, and the interaction between metal ion and the lipid is favored. This may lead to breakdown of the permeability

barrier of the cell, resulting in interference with the normal cell processes. If the geometry and charge distribution around the molecule are incompatible with the geometry and charge distribution around the pores of the bacterial cell wall, penetration through the wall by the toxic agent cannot take place and this will prevent the toxic reaction within the pores.

Chelation is not the only criterion for antibacterial activity. Some important factors such as the nature of the metal ion, nature of the ligand, coordinating sites, and geometry of the complex, concentration, hydrophilicity, lipophilicity, and the presence of co-ligands have considerable influence on antibacterial activity. Certainly, steric and pharmacokinetic factors also play a decisive role in deciding the potency of an antimicrobial agent. The presence of lipophilic and polar substituents is expected to enhance antibacterial activity. Heterocyclic ligands with multifunctionality have a greater chance of interaction either with nucleoside bases (even after complexation with metal ion) or with biologically essential metal ions present in the biosystem can be promising candidates as bactericides since they always tend to interact with enzymatic functional groups, in order to achieve higher coordination numbers [64]. Thus antibacterial property of metal complexes cannot be ascribed to chelation alone, but is an intricate blend of several contributions.

4. Conclusion

A ligand and its complexes have been synthesized and characterized by electronic absorption spectra, IR, ^{1}H NMR, and mass spectral analysis. All the metal ions are six-coordinate and the geometry can be described as octahedral. The molar conductances reveal that all the complexes are non-electrolytes. DNA-binding properties of the metal(II) complexes with DNA have been investigated by UV-Vis spectra, voltammetry, and viscosity measurements. Results indicate that the metal(II) complexes bind to CT-DNA *via* an intercalative mode. All the complexes effectively cleave plasmid DNA in the presence of oxidizing agent. DNA cleavage mechanism studies show that the complexes can promote DNA cleavage through oxidative pathway. They display higher nuclease activity for the Cu(II) complex than other complexes, so the cooperative interaction of metal ions is a factor to cleave DNA. The antimicrobial activities show that the metal complexes are more active than the ligand and Cu(II) and Zn(II) complexes are more active than the Ni(II) and Co(II) complexes.

Acknowledgments

The authors express their sincere thanks to the College Managing Board, Principal and Head of the Department of Chemistry, VHNSN College, for providing necessary research facilities. They also thank Sophisticated Analytical Instrumentation Facility, Central Drug Research Institute, Lucknow, for providing CHN analysis data, ESI-Mass, and Sophisticated Analytical Instrumentation Facility, Indian Institute of Technology, Bombay, for EPR measurements.

References

[1] J.P. Cornelissen, J.H. Van Diemen, L.R. Groeneveld, J.G. Haasnoot, A.L. Spek, J. Reedijk. *Inorg. Chem.*, **31**, 198 (1992).
[2] D.R. Richardson, P.V. Bernhardt. *J. Biol. Inorg. Chem.*, **4**, 266 (1999).
[3] D.F. Martin, G.A. Jamusonis, B.B. Martin. *J. Am. Chem. Soc.*, **83**, 73 (1961).
[4] S.N. Pandeya, D. Siram, G. Nath, E. Declercq. *Eur. J. Pharm. Sci.*, **9**, 25 (1999).
[5] R.M. Issa, S.A. Azim, A.M. Khedr, D.F. Draz. *J. Coord. Chem.*, **62**, 1859 (2009).
[6] G. Cerchiaro, K. Aquilano, G. Filomeni, G. Rotilio, M.R. Ciriolo, A.M.D.C. Ferreira. *J. Inorg. Biochem.*, **99**, 1433 (2005).
[7] J. Wang (Ed.). *Electroanalytical Techniques in Clinical Chemistry and Laboratory Medicine*, VCH, New York (1988).
[8] P.T. Kissinger, W.R. Heineman. *Laboratory Techniques in Electroanalytical Chemistry*, 2nd Edn, Marcel Dekker, New York (1996).
[9] Z.A. Siddiqi, M. Khalid, S. Kumar, M. Shahid, S. Noor. *Eur. J. Med. Chem.*, **45**, 264 (2010).
[10] X.-B. Yang, Y. Huang, J.S. Zhang, S.-K. Yuan, R.Q. Zeng. *Inorg. Chem. Commun.*, **13**, 1421 (2010).
[11] K. Serbest, A. Colak, S. Güner, S. Karaböcek. *Transition Met. Chem.*, **26**, 625 (2001).
[12] S. Mathur, S. Tabassum. *Cent. Eur. J. Chem.*, **4**, 502 (2006).
[13] J. Tan, B. Wang, L. Zhu. *Bioorg. Med. Chem.*, **17**, 614 (2009).
[14] H. Xu, K.C. Zheng, H. Deng, L.J. Lin, Q.L. Zhang, L.N. Ji. *Dalton Trans.*, **3**, 2260 (2003).
[15] V. Uma, M. Kanthimathi, T. Weyhermuller, B.U. Nair. *J. Inorg. Biochem.*, **99**, 2299 (2005).
[16] Q. Zhou, P. Yang. *Inorg. Chim. Acta*, **359**, 1200 (2006).
[17] N. Shahabadi, S. Kashanian, M. Purfoulad. *Spectrochim. Acta A*, **72**, 757 (2009).
[18] A. Sreedhara, J.A. Cowan. *J. Biol. Inorg. Chem.*, **6**, 337 (2001).
[19] S.K. Sridhar, A. Ramesh. *Biol. Pharm. Bull.*, **24**, 1149 (2001).
[20] B. Murukan, K. Mohanan. *Transition Met. Chem.*, **31**, 441 (2006).
[21] D.D. Perrin, W.L.F. Armarego, D.R. Perrin. *Purification of Laboratory Chemicals*, Pergamon Press, Oxford (1980).
[22] R.J. Angellici. *Synthesis and Techniques in Inorganic Chemistry*, W.B. Saunders Company, Philadelphia, PA (1969).
[23] M.F. Reichmann, S.A. Rice, C.A. Thomas, P. Doty. *J. Am. Chem. Soc.*, **76**, 3047 (1954).
[24] A. Wolfe, G.H. Shimer, T. Meehan. *Biochemistry*, **26**, 6392 (1987).
[25] T.B. Chaires, N. Dattaguota, D.M. Crothers. *Biochemistry*, **21**, 3933 (1982).
[26] A. Rahman, M.I. Choudhary, W.J. Thomsen. *Bioassay Techniques for Drug Development*, Harvard Academic Press, Amsterdam (2001).
[27] National Committee for Clinical Laboratory Standard Methods for Determining Bactericidal Activity of Antimicrobial Agents; Approved Guideline, M26-A, 19 (18), NCCLS, Villanova, PA (1999).
[28] P.K. Radhakrishnan. *Inorg. Chim. Acta*, **110**, 211 (1985).
[29] F. Arjmand, F. Sayeed, M. Muddassir. *J. Photochem. Photobiol. B: Biol.*, **103**, 166 (2011).
[30] M.A. Neelakantan, S.S. Marriappan, J. Dharmaraja, T. Jeyakumar, K. Muthukumaran. *Spectrochim. Acta, Part A*, **71**, 628 (2008).
[31] A.B.P. Lever. *Inorganic Electronic Spectroscopy*, 2nd Edn, Elsevier, Amsterdam (1984).
[32] F.A. Cotton, G. Wilkinson. *Advanced Inorganic Chemistry*, 5th Edn, Wiley, New York (1988).
[33] S. Chandra, R. Kumar. *Transition Met. Chem.*, **29**, 269 (2004).
[34] B.J. Hathaway, M. Duggan, A. Murphy, J. Mullane, C. Power, A. Walsh, B. Walsh. *Coord. Chem. Rev.*, **36**, 267 (1981).
[35] K. Shanker, P.M. Reddy, R. Rohini, Y.P. Ho, V. Ravinder. *J. Coord. Chem.*, **62**, 3040 (2009).
[36] P.F. Rapheal, E. Manoj, M.R.P. Kurup. *Polyhedron*, **26**, 818 (2007).
[37] B.J. Hathaway, D.E. Billing. *Coord. Chem. Rev.*, **5**, 143 (1970).
[38] B.J. Hathaway. *Struct. Bond.*, **57**, 55 (1984).
[39] S.A. Sallam. *Transition Met. Chem.*, **31**, 46 (2006).
[40] D. Kivelson, R. Neiman. *J. Chem. Phys.*, **35**, 149 (1961).
[41] B.N. Figgis. *Introduction to Ligand Fields*, Interscience, New York (1966).
[42] B.J. Hathaway, G. Wilkinson, R.D. Gillard, J.A. McCleverty (Eds.). *Comprehensive Coordination Chemistry*, Vol. 5, Pergamon, Oxford (1987).
[43] R.S. Nicholson. *Anal. Chem.*, **37**, 1351 (1965).
[44] M. Assour. *J. Chem. Phys.*, **43**, 2477 (1965).
[45] Q.L. Zhang, J.G. Liu, J. Liu, G.Q. Xue, H. Li, J.Z. Liu, H. Zhou, L.H. Qu, L.N. Ji. *J. Inorg. Biochem.*, **85**, 291 (2001).
[46] J.K. Barton, A.T. Danishefsky, J.M. Goldberg. *J. Am. Chem. Soc.*, **106**, 2172 (1984).
[47] D. Sabolová, M. Kozurkova, T. Plichta, Z. Ondrusová, D. Hudecova, M. Simkovic, H. Paulíkova, A. Valent. *Int. J. Biol. Macromol.*, **48**, 319 (2011).

[48] V.G. Vaidyanathan, B.U. Nair. *J. Inorg. Biochem.*, **94**, 121 (2003).
[49] R. Vijayalakshmi, M. Kanthimathi, V. Subramanian, B.U. Nair. *Biochim. Biophys. Acta*, **1475**, 157 (2000).
[50] N. Raman, A. Selvan. *J. Coord. Chem.*, **64**, 534 (2011).
[51] M. Patel, D. Gandhi, P. Parmar. *J. Coord. Chem.*, **64**, 1276 (2011).
[52] M.T. Carter, A.J. Bard. *J. Am. Chem. Soc.*, **109**, 7528 (1987).
[53] S.S. Zhang, S.Y. Niu, B. Qu, G.F. Jie, H. Xu, C.F. Ding. *J. Inorg. Biochem.*, **99**, 2340 (2005).
[54] S. Tabassum, S. Parveen, F. Arjmand. *Acta Biomater.*, **1**, 677 (2005).
[55] G. Psomas. *J. Inorg. Biochem.*, **102**, 1798 (2008).
[56] K. Jiao, Q.X. Wang, W. Sun, F.F. Jian. *J. Inorg. Biochem.*, **99**, 1369 (2005).
[57] S. Satyanarayana, J.C. Dabrowiak, J.B. Chaires. *Biochemistry*, **32**, 2573 (1993).
[58] J.G. Liu, Q.L. Zhang, X.F. Shi, L.N. Ji. *Inorg. Chem.*, **40**, 5045 (2001).
[59] Y. Liu, H. Chao, L. Tan, Y. Yuan, W. Wei, L. Ji. *J. Inorg. Biochem.*, **99**, 530 (2005).
[60] J.U. Rohde, J.H. In, M.H. Lim, W.W. Brennessel, M.R. Bukouski, A. Stubna, E. Munck, W. Nam, L. Que Jr. *Science*, **299**, 1037 (2003).
[61] D.P. Singh, K. Kumar, C. Sharma. *Eur. J. Med. Chem.*, **45**, 1230 (2010).
[62] B.G. Tweedy. *Phytopathology*, **55**, 910 (1964).
[63] T.J. Franklin, G.A. Snow. *Biochemistry of Antimicrobial Action*, 2nd Edn, Chapman and Hall, London (1971).
[64] P.K. Panchal, H.M. Parekh, P.B. Pansuriya. *J. Enzyme Inhib. Med. Chem.*, **21**, 203 (2006).